DOI: 10.1021/ma9025543

Macromolecules
ARTICLE

Microstructural Characterization of Poly(1-hexene) Obtained Using a Nickel α-Keto-β-diimine Initiator

Jason D. Azoulay, ‡ **Guillermo C. Bazan,** ‡ **and Griselda B. Galland*,**†

†*Instituto de Química, Universidade Federal do Rio Grande do Sul, Av. Bento Gonçalves, 9500- CEP: 91501-970 Porto Alegre, Brazil, and* ‡*Center for Polymers and Organic Solids, Departments of Chemistry & Biochemistry and Materials, University of California, Santa Barbara, California 93106*

Received November 23, 2009; Revised Manuscript Received January 16, 2010

ABSTRACT: A nickel α-keto-β-diimine initiator (**1**), when activated with methylaluminoxane (MAO) generates active sites capable of polymerizing α-olefins to high molecular weight products. Herein, we report on the full characterization and detailed microstructural analysis of poly(1-hexene) (PH) homopolymers obtained by using the **1**/MAO combination. ^{13}C NMR spectroscopy was used to provide the first qualitative and quantitative determinations of all the sequences in the poly(1-hexene). Such information yields insight into the reactivity of this novel catalytic system.

Introduction

Recent literature shows intense interest in the late transition metal (M = Ni and Pd) mediated polymerization of olefins. In contrast to early transition metal catalysts, late metal systems are more tolerant toward functionality[1−4] and may participate in "chain-walking" reactions,[5−8] in which the metal center migrates along the growing polymer chain through a series of β-hydride transfer and reinsertion steps. A wide variety of novel materials can therefore be obtained. For instance, the polymerization of ethylene by late metal cationic systems results in polyethylene (PE) ranging from a highly branched, amorphous material to a linear semicrystalline high density material afforded by variations in temperature, pressure and ligand substituents.[9] The polymerization of higher α-olefins (such as propene and 1-hexene) generally results in the production of amorphous, atactic polymers due to poor regio-selectivity and chain-end isomerization processes.[5] Control over the branch type, frequency, and mode of insertion has been achieved through variations in the ligand framework and type of monomer used and through the optimization of reaction conditions.[10−18] These distinctive features, in combination with living behavior, have led to the generation of novel materials such as elastomeric multiblock poly(α-olefins),[10] ethylene−propylene type copolymers,[19] regioblock copolymers,[20−22] and end-functionalized amorphous PE.[23]

While the microstructure of PE, polypropylene (PP)[24−26] and related materials obtained with cationic nickel systems has been well characterized, the detailed analysis of poly(1-hexene) (PH) has only been partially accomplished.[27−30] Recently, a new type of late transition metal initiator was reported, supported by the α-keto-β-diimine ligand, i.e., compound **1** in Scheme 1, which in the presence of various coactivators is capable of polymerizing α-olefins to high molecular weight products.[31] Specific conditions can be also be found such that living polymerization characterisics are attained.[32] Herein, we report on the full characterization and detailed microstructural analysis of PH homopolymers obtained using **1**/MAO. The qualitative and quantitative determination of all the polymer sequences was accomplished by using ^{13}C NMR spectroscopy and correlated with reaction mechanisms typical of cationic nickel complexes.

Scheme 1. Molecular Structure of 1 and Polymerization upon Activation with MAO

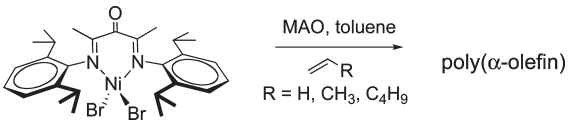

Experimental Section

The synthesis of **1** and its use in the preparation of PH homopolymers has been reported previously.[31,32] ^{13}C NMR spectra were obtained using a 300 MHz Varian Inova spectrometer. The chemical shifts were referenced internally to the methylene sequence $-(CH_2)_n-$, at 30.00 ppm. Measurements were performed in *o*-dichlorobenzene and benzene-d_6 (20% *v*/*v*) at 90 °C in a 5 mm sample tube. Spectra were taken with a 74° flip angle, an acquisition time of 1.5 s and a delay of 4.0 s.

Results

We relied on ^{13}C NMR spectroscopy to determine the microstructure of the PH obtained by the homopolymerization of 1-hexene with **1**/MAO. Three polymer samples were prepared for subsequent detailed examination. Specific details for the polymerization reactions can be found Table 1. For entries 1 and 2 (ref 31), the polymerization reactions were carried out under similar conditions, with the exception of using different reaction temperatures. Entry 1 illustrates that 1-hexene can be polymerized at 25 °C to high molecular weight product. Decreasing the reaction temperature to 0 °C leads to a PH with a narrow molecular weight distribution (PDI = 1.2) and a reduction in the overall rate of polymerization. For entry 3, optimized conditions that yield living polymerization characteristics were used. In this reaction a 300 mL reactor was loaded with 100 mL toluene and 15 mL 1-hexene ([1-hexene] = 0.85 M) and treated MAO so that [Al]/[Ni] = 250. The reaction was carried out at −10 °C. For more details see refs 31 and 32.

*Corresponding author. Fax: +55 51 33087317. Telephone: +55 51 33087304. E-mail: Griselda.barrera@ufrgs.br.

 Published on Web 02/25/2010

Table 1. Poly(1-hexene) Homopolymers Obtained Using 1/MAO with Data from References 31 and 32

entry[a]	conditions[b]	TOF[c]	M_n[d]	PDI	T_g[e]
1/10	250 MAO, 25 °C, 10 mL 1-hexene, 60 min	356	120	2.0	−56
2/10	250 MAO, 0 °C, 10 mL 1-hexene, 60 min	89	157	1.2	−55
3/12.5[f]	250 MAO*, −10 °C, 15 mL 1-hexene, 120 min	300	120	1.05	−62

[a] Units: μmoL of **1**. [b] Entries 1−2 carried out in a Schlenk flask in 10 mL toluene at a [1-hexene] = 4 M. In entry 3 [1-hexene] = 0.85 M. [c] Units: h^{-1}. [d] Units: $\times 10^{-3}$ g mol^{-1} determined by GPC in *o*-dichlorobenzene at 135 °C as determined by GPC versus polystyrene standards. M_n values calculated on the basis of TOF are lower than those shown and indicate that the use of polystyrene standards substantially overestimates the M_n for entries 1−3. [e] °C. [f] In entry 3, the volatiles were removed from a commercially available MAO solution.

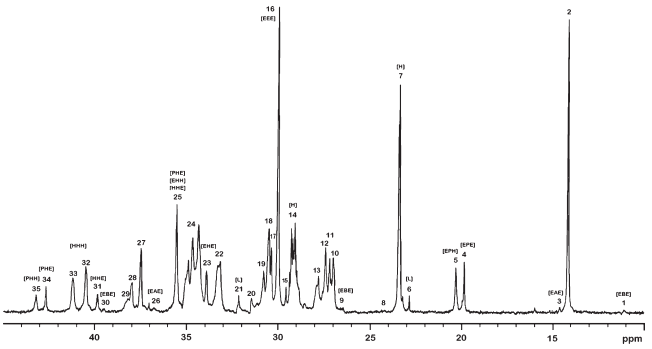

Figure 1. ^{13}C NMR spectrum of the poly(1-hexene) obtained in entry 1.

Spectroscopic assignments were based on APT−^{13}C (attached proton test) NMR spectra, theoretical chemical shifts calculated by Lindemann and Adams[33] and previous assignments.[24−29,34−38] Branches are named by *x*B*n*, where *n* is the length of the branch and *x* is the carbon number starting with the methyl group as "1". Greek letters and "br" are used instead of *x* for the methylenes and the branch point, respectively.[26] For paired branches, prefixes "1,*m*" are used, where *m* is the number of carbons between two tertiary carbons; 1 being the first tertiary carbon and *m* the next. The backbone carbons between branches are designated by Greek letters with primes. The ^{13}C NMR spectrum of the PH obtained in entry 1 is shown in Figure 1. All the peaks have been assigned, which to our knowledge has not been done for this type of branched PH. In Table 2, the peak numbers corresponding to Figure 1 are shown in the first column. The second and third columns provide the calculated and experimentally determined chemical shifts, respectively; while column 4 shows the carbon atom assignment. The last column shows the triad sequences using the copolymer nomenclature. In this nomenclature, an ethylene unit is designated by the letter E, a propyl unit with P, which corresponds to a methyl branch; B, a butyl unit corresponding to an ethyl branch; A, an amyl unit corresponding to a propyl branch; H, a hexyl unit corresponding to a butyl branch and L, a $CH_2CH(CH_2)_nCH_3$ ($n > 3$) unit corresponding to a longer branch. The inverted unit is marked by an "∗". The APT−^{13}C experiment of the same sample, where the carbon signals of even multiplicity (methylene carbons) appear 180° opposite in phase with respect to carbon signals of odd multiplicity (methyl and methine carbons) is shown in Figure 2 and was used to confirm the assignments.

Using Table 2 below, the identified triads were related to peak integrals or combinations of them. Whenever possible the average of two or more peaks representing the sequence was used.

The equations used in the quantitative analysis of the poly(1-hexene) are listed below:

$$[E] = [EEE] + [HEH] + [PEE + EEP] + [EEH + HEE] + [EEB + BEE] + [EEA + AEE] + [EEL + LEE] = I_{16}/2 + I_8 + I_{10} + I_{11} + I_{12}$$

$$[HEH] = I_8$$

$$[EEH(H) + (H)HEE] = I_{10}$$

$$[EEB + BEE] + [EEA + AEE] + [EEH + HEE] + [EEL + LEE] = I_{11}$$

$$[EEP + PEE] = I_{12}$$

$$[HEEP*] + [PEEP*] = I_{13}/2$$

$$[EEE] = I_{16}/2$$

$$[EH*H] = I_{20}/2$$

$$[P] = [EPE] + [EPH] = I_4 - I_3 + I_5$$

$$[EPE] = I_4 - I_3$$

$$[EPH] = I_5$$

$$[B] = [EBE] = (I_1 + I_{30})/2$$

$$[A] = [EAE] = (I_3 + I_{26})/2$$

$$[H] = [EHE] + [HHH] + [HHE + EHH] + [PHH] + [PHE] = (I_7 + I_{14})/2$$

$$\text{or} \quad I_{23} - I_1 - I_{30} + I_{22} - I_4 + I_3 + I_{25}$$

$$[EHE] = I_{23} - I_1 - I_{30}$$

$$[HHH] + [PHH] = I_{22} - I_4 + I_3$$

$$[HHH] = I_{22} - I_4 + I_3 - I_{35}$$

$$[(H)HHH] = I_{33}$$

$$[(E)HHH] = I_{22} - I_4 + I_3 - I_{35} - I_{33}$$

$$[HHE + EHH] = (E)HHE + (H)HHE = (I_{25} - I_{34})$$

$$[PHH] = I_{35}[PHE] = I_{34}$$

$$[L] = [ELE] = (I_6 + I_{21})/2$$

The results of the application of the above equations are presented in Table 3, where the sequences are expressed as the percentage of total sequences. The ^{13}C NMR spectra of the three samples are shown in Figure 3. NMR data can also be expressed in terms of the percent of a given branch relative to the total branches, as in Table 4. The only ambiguity is the number of carbon atoms in a long branch. Most of the carbon signals arising from a long branch appear at 30.00 ppm and are included in the $(EEE)_n$ sequence. The only carbons that appear out of these sequences are $1B_n$, $2B_n$, $3B_n$, $4B_n$, $(n-2)B_n$, $(n-1)B_n$, nB_n, brB_n and αB_n, which correspond to 1 C each. The βB_n and γB_n carbons are already included in [E] as sequences EEL + LEE. Thus, we can multiply [L] by 9 to include long branches in the equation below. To convert NMR-determined values to branches per 1000 carbon atoms it is necessary to obtain the total number of carbons

Table 2. Poly(1-hexene) ^{13}C Nuclear Magnetic Resonance Results, Calculated and Observed Chemical Shifts and Assignments

	chem. shift (ppm)			
peak no.	calcd	expt	assignments	sequences
1	11.36	11.10	$1B_2$	[EBE]
2	13.86	14.15	$1B_4$, $1B_n$	[EHE] + [HHH] + [HHE + EHH] + [PHH] + [PHE] + [ELE]
3	14.35	14.60	$1B_3$	[EAE]
4	19.63	19.85	$1B_1$	[EPE]
	20.21	20.00	$2B_3$	[EAE]
5	20.12	20.30	$1B_1$	[EPH]
6	22.65	22.86	$2B_n$	[ELE]
7	22.90	23.30−23.45	$2B_4$	[EHE] + [HHH] + [HHE + EHH] + [PHH] + [PHE]
8	25.08	24.1−24.4	$\beta\beta B_4$	[HEH]
9	27.16	26.51	$2B_2$	[EBE]
10	27.52	26.9−27.1	βB_4	[E*E*HH + HH*E*E]
11		27.17	βB_2, βB_3, βB_4, βB_n, $(n-1)B_n$,	[EEB + BEE] + [EEA + AEE] + [EEH + HEE] + [EEL + LEE]
12	27.27	27.41	βB_1	[EEP + PEE] + [EEP(H)]
13	27.77	27.79	1,6-$\beta' B_{4-n}B_1$	[HEEP*] + [PEEP*]
14	29.96	28.5−29.5	$3B_4$	[EHE] + [HHH] + [HHE + EHH] + [PHH] + [PHE]
15	29.71	29.59	$4B_n$	[ELE]
16	29.96	30.00	δB_{1-n}	[EEE]
17	30.21	30.36	γB_1	[EEP]
18	30.21	30.50	γB_{2-n},	[EEB] + [EEH] + [EEA] + [EEL]
			$(n-2)B_n$	[ELE]
19	30.45	30.71	brB_1	[EPH]
20	32.03	31.44	1,4-$\alpha' B_{4-n}$	[EH*H]
21	32.40	32.15	$3B_n$	[ELE]
22	32.52	33.0−33.5	brB_1	[EPE]
	32.91		brB_4	[HHH] + [PHH]
23	34.22	33.88	$4B_4$	[EHE]
			αB_2	[BEE] + [EBE]
24	34.47	34.1−35.2	αB_4	[EH*E*E] + [EE*H*E]
			$4B_4$	[EHH + HHE] + [PHE]
			1,6-$\alpha' B_{4-n}$	[H*E*EH*] + [H*E*EP*]
			αB_n, $(n-1)B_n$	[EL*E*E] + [EE*L*E]
			αB_3	[EAE]
	34.72		$4B_4$	[HHH] + [PHH]
			αB_4	[EE*H*H] + [HH*E*E]
			$\alpha\gamma B_4$	[HE*H*E] + [EH*E*H]
	34.97		$\alpha\gamma B_4$	[HE*H*H] + [HH*E*H]
25	34.98	35.46	brB_4	[EHH + HHE] + [PHE]
26	36.91	36.72	$3B_3$	[EAE]
27	36.91	37.47	αB_1	[EPE] + [EP*E*E]
			1,6-$\alpha' B_1$	[P*E*EP*]
28	37.05	37.93	brB_{3-n}	[EHE]+ [ELE]+ [EAE]
			1,4-brB_4	[EH*H]
29	37.16	38.0−38.3	αB_1	[(E)E*P*H]
30	39.12	39.44	brB_2	[EBE]
31	38.98	39.73	$\alpha\alpha B_4$	[(E)H*H*E]
32	39.23	40.32	$\alpha\alpha B_4$	[(H)HHE] + [(E)H*H*H]
33	39.48	41.08	$\alpha\alpha B_4$	[(H)HHH]
34	41.42	42.61	$\alpha\alpha B_4$	[(E)P*H*E]
35	41.67	43.14	$\alpha\alpha B_4$	[(E)P*H*H]

present from each sequence, which can be done using the following equation:

$$\text{total number of carbon atoms} = [\text{E}] \times 2 + [\text{P}] \times 3 + [\text{B}] \times 4 + [\text{A}] \times 5 + [\text{H}] \times 6 + [\text{L}] \times 9$$

$$\text{CH}_3/1000\text{C} = ([\text{branch[P] or etc.}])/\text{total no. of carbon atoms}) \times 1000$$

This result for the samples studied is listed in the last three column of Table 4.

Discussion

The polymerization of 1-hexene with **1**/MAO produces a regioirregular polymer with backbone methylene sequences of various lengths with methyl, ethyl, propyl, butyl and long side chains. Scheme 2 provides a reasonable route to the formation of different branch types together with the corresponding sequence.

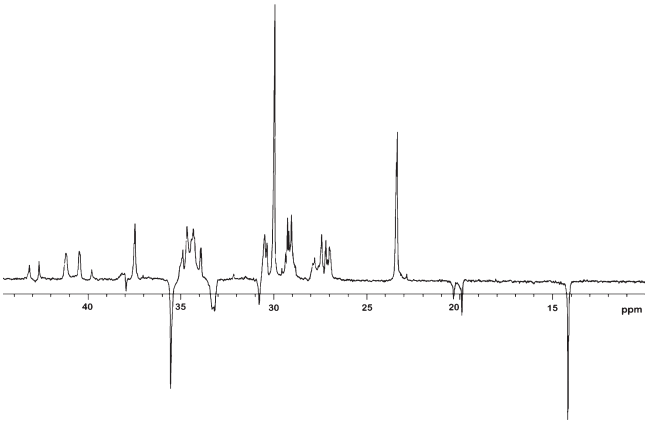

Figure 2. APT−^{13}C NMR spectrum of the poly(1-hexene) obtained in entry 1.

Table 3. Percentage of Monomer Sequences in mol % of the Poly(1-hexene) Obtained at Different Reaction Temperatures and Concentrations

	monomer sequences (mol %)		
sequences	entry 1[a]	entry 2[a]	entry 3[b]
[E]	**48.4**	**41.9**	**55.9**
[HEH]	0.0	0.0	8.5
[EEHH + HHEE]	10.9	14.4	6.4
[EEB + BEE] + [EEA + AEE] + [EEH + HEE] + [EEL + LEE]	6.3	4.8	14.9
[EEP + PEE]	12.8	8.2	10.3
[PEEP[a]] + [HEEP[a]]	4.7	2.8	0.6
[EEE]	18.5	14.5	15.8
[EEP]	7.0	4.2	6.3
[EEB] + [EEH] + [EEA] + [EEL]	15.1	18.2	13.8
[EH[a]H]	1.4	1.4	2.0
[P] = [EPE] + [EPH]	**11.6**	**6.6**	**7.1**
[EPE]	5.4	3.3	4.7
[EPH]	6.2	3.3	2.4
[B] = [EBE]	**0.3**	**0.8**	**0.3**
[A]=[EAE]	**0.7**	**0.4**	**0.9**
[H] = [EHE] + [HHH] + [HHE + EHH] + [PHH] + [PHE]	**37.3**	**48.4**	**34.6**
[EHE]	4.9	3.8	15.2
[HHH] + [PHH]	14.2	27.3	6.0
[HHH] = [(H)HHH + (E)HHH)	10.7	25.3	6.0
[(H)HHH]	8.0	18.0	2.1
[(E)HHH]	2.7	7.3	3.9
[(H)HHE] + EHH	13.4	12.8	7.4
[(E)HHE	2.1	3.2	4.8
[HHE + EHH] = (E)HHE + (H)HHE + EHH	15.5	16.0	12.1
[PHH]	3.5	2.0	0.0
[PHE] =	2.7	1.2	1.2
[L] = [ELE]	**1.7**	**2.0**	**1.2**
[E] + [P] + [B] + [A] + [H] + [L]	100.0	100.0	100.0

[a][1-hexene] = 4 M. [b][1-hexene] = 0.85 M.

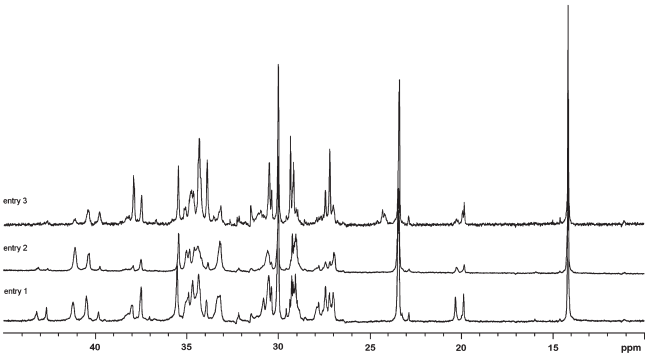

Figure 3. ^{13}C NMR spectra of entries 1−3.

The presence of different branch types can be explained as a result of the regiochemistry of monomer insertion (1,2 or 2,1-insertion of the 1-hexene monomer into the Ni−polymer bond), and the ability of the metal center to migrate along the growing polymer chain via a series of (formal) β-hydride elimination and reinsertion steps. Butyl branches predominate and arise as a result of chain growth by successive 1,2-insertions, which correspond to the HHH sequence, as depicted in Scheme 1. That butyl branches predominate is consistent with the rate of insertion/propagation being faster than migration. Methyl branches of the type PHH, EPH, and EEP arise as a result of 1,2-insertion into **2** to give **3**, followed by migration and formation of **5**.

Ethyl and Propyl Branches. Resonances arising from ethyl and propyl branches, which constitute a small percentage of the branch type, were detected. The resonances associated with ethyl branches appear at 11.10 ppm ($1B_2$, peak 1), 26.51 ppm ($2B_2$, peak 9), and 39.44 ppm (brB_2, peak 30), and correspond to the [EBE] sequence. Propyl branches are represented by the peaks at 14.60 ppm ($1B_3$, peak 3) and at 36.72 ppm ($3B_3$, peak 26), however, other resonances associated with propyl branches are occluded by resonances arising from $1B_1$ (peak 4) and brB_4 (peak 28). Ethyl and propyl branching is the result of 2,1-insertion into **2** to give **10** followed by successive elimination and reinsertion steps, which ultimately result in **15** and **13** respectively. Because of the fact that a 2,1-insertion of a new unit or a 1,2-insertion in a secondary carbon is not very probable, these branches are isolated between ethylene units giving [EBE] and [EAE] sequences.

Table 4. Type and Amount of Branches Given as a Percentage of the Total Branches and Branches per 1000 Carbon Atoms

	(mol %)			CH_3/1000 C		
branch type	−10 °C	0 °C	+25 °C	−10 °C	0 °C	+25 °C
methyl	16.1	11.4	22.5	20	16	31
ethyl	0.7	1.4	0.5	1	2	1
propyl	2.0	0.7	1.4	3	1	2
butyl	78.4	83.2	72.4	96	116	99
long	2.8	3.4	3.2	3	5	4
total	100.0	100.0	100.0	123	140	137

Long Branches. Resonances associated with long branches, denoted by the sequence [ELE], and used to distinguish between butyl branches, can be seen in the ^{13}C NMR spectrum at 22.86 ppm ($2B_n$, peak 6) and 32.15 ppm ($3B_n$, peak 21). The presence of long branches isolated between ethylene units arise as a result of 2,1-insertion into **5** to give **8**, metal migration to the primary carbon and subsequent enchainment to give **9**.

Methyl branches. Methyl branches of the type [PHH], [EPH], and [EEP] arise from 1,2-insertion into **2** to give **3**, followed by 2,6-enchainment to give **5**. A subsequent

Scheme 2. Proposed Mechanism of Branch Formation

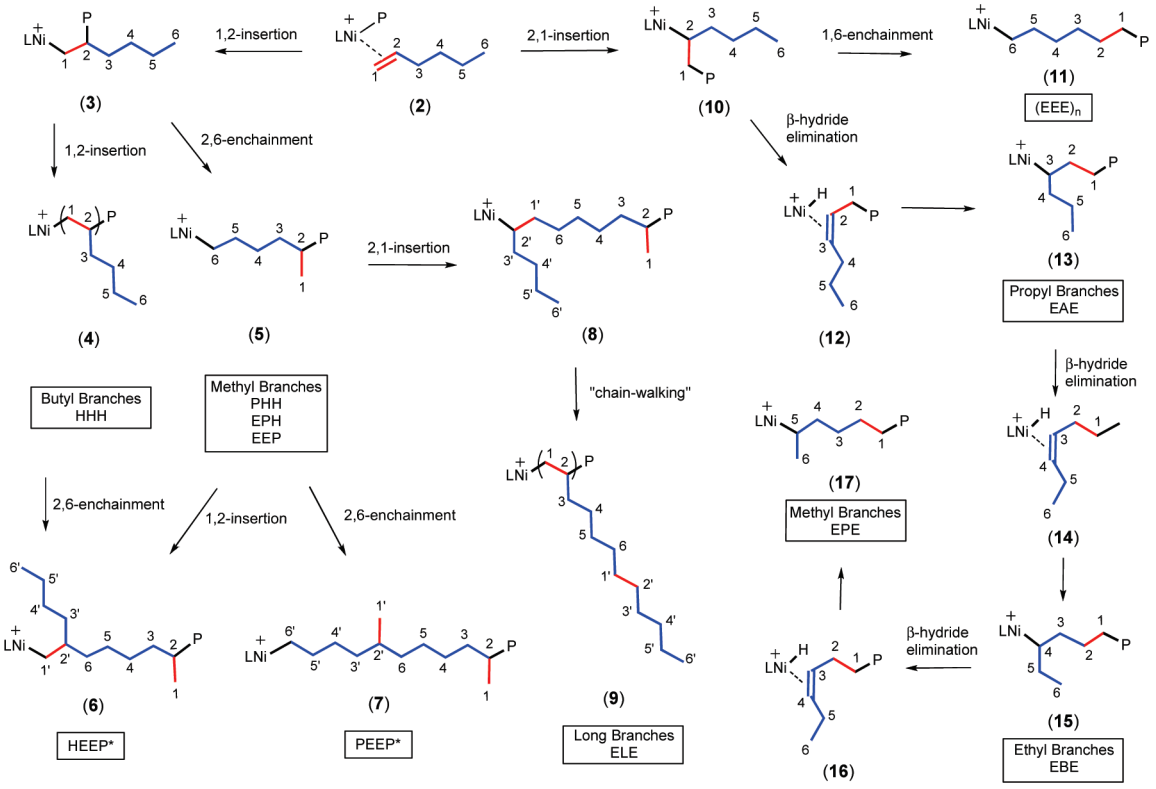

1,2-insertion into **5** leads to a methyl branch 4 methylene units away from a butyl branch, giving rise to the **6** (1,6-B_4B_1 or HEEP* sequence). 2,6-Enchainment by **5**, gives rise to two methyl branches separated by 4 methylene units to give **7** (1,6-B_1B_1 or PEEP* sequences). The carbon $\beta'B_{1\text{-}n}$ from these sequences appears at 27.79 ppm (peak 13). Another way that methyl branches can be introduced is through an initial 2,1-insertion of the monomer into **2**, which results in **10**. Successive elimination and reinsertion steps result in a larger numbers of methylene units in the polymer backbone and isolated methyl branches of the type [EPE], structure **17**. The characteristic resonance associated with these branches can be observed at 19.85 ppm (resonance 4, $1B_1$). The resonance associated with the brB_1 carbon atom (33.17 ppm) is occluded by the brB_4 resonance from butyl branches (peak 22).

Chain walking cannot be used to explain the resonance associated with two methyl branches separated by one methylene atom as in the EPP + PPE sequence. This resonance, can be unambiguously distinguished in the spectrum and appears at 20.30 ppm (peak 5) from $1B_1$ and at 30.71 (peak 19) from brB_1.[28] These peaks can be assigned to sequences of the type [EPH], that are formed by successive 1,2-insertions followed by 2,6-enchainment, which generates a methyl branch followed by ethylene units. Methyl and methine carbons from these sequences appear at the same frequencies as those of EPP + PPE sequences, but $\alpha\alpha B_1$ methylene carbons appear at 45.0 - 47.7 ppm[25] for the PPE sequence, which was not detected in our sample. The $\alpha\alpha B_1B_4$ carbon atom of sequences (E)P*H*E and (E)P*H*H can be assigned at 42.61 (peak 34) and 43.14 ppm (peak 35), respectively. The integrated peak area corresponding to triad EPH is anticipated to follow the following relationship:

$$\text{EPH} = \text{PPH} + \text{PHE}, \quad I_5 = I_{34} + I_{35}$$

This relationship is strictly followed by the PH obtained at 0 and 25 °C, but in the PH obtained at −10 °C, the PHH triad is nonexistent and the peak area of the triad EPH is marginally larger than that of PHE triad showing an ambiguity in this sample.

Butyl Branches. Butyl branches arise from successive 1,2-insertions into **2** giving [HHH] sequences and are assigned in accord with the literature.[34,35] The total amount of butyl branches can be calculated from carbon atoms $2B_4$ and $3B_4$ at 23.30−23.45 ppm (peak 7) and 28.5−29.5 ppm (peak 14), respectively and also by addition of the following triads: EHE + HHH + PHH + HHE + EHH + PHE (see quantitative equations). The discrepancy between both results for the sample produced at low temperature is less than 5%, and only in the case of the sample made at 25 °C is the error is close to 10%, which is quite reasonable given the experimental error in resonance integrals. The region at 26.9 - 27.1 ppm (peak 10) is due to sequences of the type HHEE + EEHH with different tacticities. The presence of triads of the type EHH + HHE and PHE are seen at 35.46 ppm (peak 25) from the tertiary carbon brB_4. APT−^{13}C NMR spectroscopy shows that this resonance belongs only to a tertiary carbon atom. This assignment excludes the possibility that this peak is generated by isotactic sequences of the type [HHH]*mm* or [HHE + HHE]*m* from the $4B_4$ carbon as previously reported.[34,36] This excludes the possibility of isotactic HHH sequences in these samples. Atactic and syndiotactic resonances of these sequences appear in the 34.1 − 35.2 ppm region (peak 24) due to carbon atoms $4B_4$ and αB_4.

The $4B_4$ carbon atom from the EHE sequence appears at 33.88 ppm (peak 23). Peak 11 arises from a butyl branch of the type EEH + HEE, although other triads due to the β carbon of other branches appear in this region at low intensity. Sequences of the type PHH come from a series of 1,2-insertions into **2** to give **3** followed by 2,6-enchaiment to give **5**. Sequences of the type PHP that are not distinguishable from HHH or PHH sequences and may be

disregarded as there is no mechanistic rationale for their existence. Thus, resonances of carbon atoms $\alpha\alpha B_4$ at 40.32 (peak 32) and 41.08 ppm (peak 33) are assigned to HHH sequences.

The presence of a resonance at 31.44 ppm (peak 20) can only be attributed to the 1,4-$\alpha'B_4$ carbon atom (EH*H) implying that few 2,1-insertions can follow 1,2-insertion without rearrangement. This is more pronounced at reduced reaction temperatures as their occurrence at −10 °C is higher than at 0 or 25 °C.

In the polymerization performed at −10 °C (entry 3), there is a resonance at 24.1 −24.4 ppm that is not present in the products obtained at the higher temperatures. Because of the high intensity of this peak (8.6 mol %), this resonance can only be attributed to carbon $\beta\beta B_4$ arising from a [HEH] sequence. Chain walking does not explain the existence of this sequence and further studies will be necessary to explain the presence of this resonance.

Ethylene Sequences. Signals arising from ethylene sequences at 30.00 ppm come from 2,1-insertion into **2** to give **10**, followed by 1,6-enchaiment to give **11** and from long branches (i.e., **9**). It is not possible to distinguish between both type of $(CH_2)_n$ sequences.

Tacticity. The resonances associated with tacticity, carbons $3B_4$, $4B_4$, and $\alpha\alpha B_4$ at 28.5−29.5 (peak 14), 34.1−35.2 (peak 24), 40.32 (peak 32), and 41.08 ppm (peak 33) respectively, exhibit a complex structure that corresponds to an atactic arrangement of butyl branches. Because of the overlapping of these signals it is difficult to specify tacticity.

Temperature Effects. The PH obtained from the reactions carried out at 0 and 25 °C (entries 2 and 1 in Table 1) were performed under the same reaction conditions and monomer concentration ([1-hexene] = 4 M) and therefore serve as useful materials to probe the effect of termperature. Butyl branching decreases from 48.4 mol % to 37.3 mol % (Table 4) when the temperature is increased, as determined by a decrease in the HHHH sequence from 18.0 to 8.0 mol %. One can conclude that at elevated temperatures 1,2-insertion of the monomer becomes less favored. On the other hand, methyl branching increases from 6.6 mol % (0 °C) to 11.6 mol % (25 °C). Signals corresponding to the sequences associated with methyl branching of the type (EPE and EPH) show a significant increase, which illustrates that an increase in temperature accelerates 2,6-enchainment and chain walking processes. Other branches (ethyl, propyl and long branches) are present in less than 2.0 mol % and do not exhibit a clear trend.

Monomer Concentration Effect. Comparison of the PH obtained at −10 °C ([1-hexene] = 0.85 M) versus that obtained at 0 °C ([1-hexene] = 4 M) illustrates that the total butyl branching is lower for the polymer obtained at a lower temperatures and under these conditions. This suggests that concentration may have important implications in the resultant structure of the material. Sequences of the type HHHH decrease from 18.0 (0 °C) to 2.1 (−10 °C) mol %, which is consistent with a lower tendency toward propagation at lower 1-hexene concentrations. This result is expected because a higher concentration of 1-hexene should favor normal (1,2) propagation reactions ($R_p \propto k_p[H]$).[27] Sequences of the type EHE, resulting from 2,1-insertion, followed by 1,6-enchainment or chain walking increase significantly from 3.8 mol % (0 °C) to 15.2 mol % (−10 °C). Increasing the reaction temperature from 0 to 25 °C at [1-hexene] = 4 M resulted in no change in this feature. As the monomer concentration and temperature are decreased, there is a substantial increase in methyl branching. The appearance of methyl branching is more sensitive to monomer concentration than reaction temperature, as noted by comparison of the reactions carried out at 0 and −10 °C. It seems that at lower monomer concentrations chain walking reactions are more likely. Other branches are present in low amount (< 1.2 mol %) and variations fall within experimental error. The amount of ethylene sequences increases significantly in the PH obtained at −10 °C as noted by an increase of the EEH + HEE sequences that are a consequence of the higher fractions of EHE sequence. It is interesting to note that there are a significant amount of sequences of the type HEH (8.5 mol %) present in the sample obtained at −10 °C that are not present in the other samples. The presence of sequences of the type HEH will merit further study, as these sequences are difficult to account for within a standard chain-walking rationale.

Conclusion

The structure of various PH homopolymers obtained under different reaction conditions utilizing the **1**/MAO catalyst combination were quantitatively and qualitatively characterized using ^{13}C NMR spectroscopy. New sequences such as EPH have been assigned and correlated with generally accepted transition metal mediated mechanisms. A simple method to calculate the amount of each monomer sequence has been developed. Insight into the reaction mechanism and factors affecting polymer microstructure have been elucidated. Temperature and monomer concentration effects are in-line with previous observations in that increasing the reaction temperature and decreasing the monomer concentration favor migration over propagation. Monomer concentration seems to have a stronger influence than reaction temperature.

Acknowledgment. The authors thanks to Conselho Nacional de Desenvolvimento Científico e Tecnológico (CNPQ) and Department of Energy for financial support.

Supporting Information Available: Table 1S, showing quantitative self-consistency check between experimental resonance integrals with the integrals calculated by quantitative equations. This material is available free of charge via the Internet at http://pubs.acs.org.

References and Notes

(1) Johnson, L. K.; Mecking, S.; Brookhart, M. *J. Am. Chem. Soc.* **1996**, *118*, 267–268.
(2) Mecking, S.; Johnson, L. K.; Wang, L.; Brookhart, M. *J. Am. Chem. Soc.* **1998**, *120*, 888–899.
(3) Younkin, T. R.; Conor, E. F.; Henderson, J. I.; Friedrich, S. K.; Grubbs, R. H.; Bansleban, D. A. *Science* **2000**, *287*, 460–462.
(4) Berkefeld, A.; Mecking, S. *Angew. Chem., Int. Ed.* **2008**, *47*, 2–7.
(5) Johnson, L. K.; Killian, C. M.; Brookhart, M. *J. Am. Chem. Soc.* **1995**, *117*, 6414–6415.
(6) Ittel, S. D.; Johnson, L. K.; Brookhart, M. *Chem. Rev.* **2000**, *100*, 1169–1203.
(7) Guan, Z.; Cotts, P. M.; McCord, E. F.; McLain, S. J. *Science* **1999**, *283*, 2059–2062.
(8) Leatherman, M. D.; Svedja, S. A.; Johnson, L. K.; Brookhart, M. *J. Am. Chem. Soc.* **2003**, *125*, 3068–3081.
(9) Meinhard, D.; Wegner, M.; Kipiani, G.; Hearley, A.; Reuter, P.; Fischer, S.; Marti, O.; Rieger, B. *J. Am. Chem. Soc.* **2007**, *129*, 9182–9191.
(10) Killian, C. M.; Tempel, D. J.; Johnson, L. K.; Brookhart, M. *J. Am. Chem. Soc.* **1996**, *118*, 11664–11665.
(11) Ittel, S. D.; Johnson, L. K.; Brookhart, M. *Chem. Rev.* **2000**, *100*, 1169–1203.
(12) Camacho, D. H.; Salo, E. V.; Ziller, J. W.; Guan, Z. *Angew. Chem., Int. Ed.* **2004**, *43*, 1821–1825.
(13) Camacho, D. H.; Guan, Z. *Macromolecules* **2005**, *38*, 2544–2546.

(14) Leung, D. H.; Ziller, J. W.; Guan, Z. *J. Am. Chem. Soc*. **2008**, *130*, 7538–7539.
(15) Rose, J. M.; Cherian, A. E.; Lee, J. H.; Archer, L. A.; Coates, G. W.; Fetters, L. J. *Macromolecules* **2007**, *40*, 6807–6813.
(16) Stapleton, R. A.; Chai, J.; Nuanthanom, A.; Flisak, Z.; Nele, M.; Ziegler, T.; Rinaldi, P. L.; Soares, J. B. P.; Collins, S. *Macromolecules* **2007**, *40*, 2993–3004.
(17) Gottker-Schnetmann, I.; Wehram, P.; Rohr, C.; Mecking, S. *Organometallics* **2007**, *26*, 2348–2362.
(18) Azoulay, J. D.; Itigaki, K.; Wu, G.; Bazan, G. C. *Organometallics* **2008**, *27*, 2273–2280.
(19) Rose, J. M.; Cherian, A. E.; Coates, G. W. *J. Am. Chem. Soc*. **2006**, *128*, 4186–4187.
(20) Cherian, A. E.; Rose, J. M.; Lobkovsky, E. B.; Coates, G. W. *J. Am. Chem. Soc*. **2005**, *127*, 13770–1377.
(21) Rose, J. M.; Deplace, F.; Lynd, N. A.; Wang, Z.; Hotta, A.; Lobkovsky, E. B.; Kramer, E. J.; Coates, G. W. *Macromolecules* **2008**, *41*, 9548–9555.
(22) Rose, J. M.; Cherian, A. E.; Coates, G. W. *J. Am. Chem. Soc*. **2006**, *128*, 4186–4187.
(23) Gottfried, A. C.; Brookhart, M. *Macromolecules* **2003**, *125*, 3085–3100.
(24) McCord, E. F.; McLain, S. J.; Nelson, L. T. J.; Arthur, S. D.; Coughlin, E. B.; Ittel, S. D.; Johnson, L. K.; Tempel, D.; Killian, C. M.; Brookhart, M. *Macromolecules* **2001**, *34*, 362−3; 71.
(25) Galland, G. B.; Da Silva, L. P.; Dias, M. L.; Crosetti, G. L.; Ziglio, C. M.; Filgueiras, C. A. L. *J. Polym. Sci: Part A: Polym. Chem*. **2004**, *42*, 2171–2178.
(26) Galland, G. B.; de Souza, R. F.; Mauler, R. S.; Nunes, F. F. *Macromolecules* **1999**, *32*, 1620–1625.
(27) Peruch, F.; Cramail, H.; Deffieux, A. *Macromolecules* **1999**, *32*, 7977–7983.
(28) Subramanyam, U.; Rajamohanan, P. R.; Sivaram, S. *Polymer* **2004**, *45*, 4063–4076.
(29) Yuan, J. C.; Silva, L. C.; Gomes, P. T.; Valerga, P.; Campos, J. M.; Ribairo, M. R.; Chien, J. C. W.; Marques, M. M. *Polymer* **2005**, *46*, 2122–2132.
(30) Merna, J.; Cihlar, J.; Kucera, M.; Deffieux, A.; Cramail, H. *Eur. Polym. J*. **2005**, *41*, 303–312.
(31) Azoulay, J. D.; Rojas, R. S.; Serrano, A. V.; Ohtaki, H.; Galland, G. B.; Bazan, G. C. *Angew. Chem., Int. Ed. Engl*. **2009**, *48*, 1089–1092.
(32) Azoulay, J. D.; Schneider, Y.; Galland, G. B.; Bazan, G. C. *Chem. Commun*. **2009**, *41*, 6177–6179.
(33) Linderman, L. P.; Adams, J. Q. *Anal. Chem*. **1973**, *43*, 1245–1252.
(34) Randall, J.C. Rev. *Macromol. Chem. Phys*. **1989**, *29*, 201–317.
(35) Escher, F. F. N.; Galland, G. B. *J. Polym. Sci., Part A: Polym. Chem*. **2004**, *42*, 2474–2482.
(36) Galland, G. B.; Da Silva, L. F.; Nicolini, A. *J. Polym. Sci., Part A: Polym. Chem*. **2005**, *43*, 4744–4753.
(37) Asakura, T.; Demura, M.; Nishiyama, Y. *Macromolecules* **1991**, *24*, 2334–2340.
(38) Forlini, F.; Tritto, I.; Locatelli, P.; Sacchi, M.; Piemontesi, F. *Macromol. Chem. Phys*. **2000**, *201*, 401–408.